H1-08/97-527

Study of Photoproduction Processes at HERA

A.I.Lebedev (for the H1 and ZEUS Collaborations)

P.N.Lebedev Physical Institute, Academy of Sciences of Russia
Leninsky Prospect 53, 117924 Moscow, Russia

Talk given at the XI International Workshop
on High Energy Physics and Quantum Field Theory
St.Petersburg, Russia, September 12 - 18, 1996

Abstract

The H1 and ZEUS recent results in the investigation of soft and hard photoproduction processes at the ep-collider HERA are presented and discussed. The studies of the photoabsorption, inclusive particle spectra, jet photoproduction, diffraction and charm production have clarified the phenomenology and parton dynamics of γp-interactions and revealed their resemblance to and distinction from hadron reactions.

1 Introduction

The collisions of $27.5GeV$ electrons (or the positrons) with protons of energy $E_p = 820GeV$ at ep-collider HERA provides the unique possibility for the study of hadron photoproduction processes

$$\gamma + p \to hadrons \tag{1}$$

at extremely high energies up to $48TeV$ in the rest system of proton (300 GeV in the center of mass system - c.m.s.) which is not accessible at fixed target accelerators. The investigations of these reactions have a goal to stimulate the developments on high energy physics models, check VDM [1] and QCD (see *e.g.* [2]) approaches and search for the manifestation of new physics.

HERA accelerator has two interaction points for ep-collisions (North and South) where two multi-purpose detectors - H1 [3] and ZEUS [4] respectively - are placed. Both of them contain electromagnetic and hadronic calorimeters and central tracking systems placed in a strong magnetic field (1.1-1.5$Tesla$) which is produced by superconducting solenoids. This equipment is surrounded by sliced steel construction which serves as magnet return yoke and muon filter at the same time.

The electromagnetic ep-interaction is mediated by the exchange of a photon (Fig.1) with negative

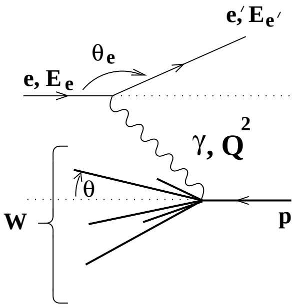

Figure 1: Kinematics of hadron production in ep-scattering.

squared 4-momentum Q^2 and energy fraction y which are equal for small deflections of electron from the initial direction to

$$Q^2 = 4E_eE_{e'}\cos^2(\frac{\theta_e}{2}) \approx E_eE_{e'}(\pi - \theta_e)^2, \tag{2}$$

$$y = 1 - \frac{E_{e'}}{E_e}\sin^2(\frac{\theta_e}{2}) \approx 1 - \frac{E_{e'}}{E_e} = \frac{E_\gamma}{E_e}. \tag{3}$$

Here θ_e is the angle of electron scattering counted for the HERA case from the direction of the incoming proton, E_e and $E_{e'}$ are electron energies before and after scattering, E_γ is the energy of the intermediate photon. The final hadron system is characterized by the total energy in the γp-c.m.s. $W = 2\sqrt{E_\gamma E_p}$ and by the angle of hadron emission θ or by its pseudo-rapidity $\eta = -\ln\tan(\theta/2)$. At low Q^2 the intermediate photon is almost real and the electroproduction reaction study gives information on the processes (1). Williams-Weizsäcker (WW) approximation [5] with some corrections [6] is used to obtain the photoproduction cross section from the measured ep-scattering cross section.

When the recoil electron stays after scattering in the beam pipe and is not detected the virtual photon has $Q^2 < 4GeV^2$ [1]. For reactions induced by such a photon (so called untagged photoproduction events) the average Q^2 value is of $0.2GeV^2$. It is possible also to fix small Q^2 values by tagging the recoil electrons in e-counters of the luminosity measurement system. For these tagged photoproduction events $Q^2 < (0.01 - 0.02)GeV^2$. In the case of tagged events y (and W) is determined directly from the relation (3). For untagged photoproduction it is calculated with help of the Jacquet-Blondel relation [7] using information on the final hadronic state: $y = \Sigma_i(E_i - p_{i,z})/2E_e$ where E_i is the energy of the final hadron and $p_{i,z}$ is the projection of its momentum on the direction of initial proton beam.

In the subsequent sections the recent results on the studies of soft and hard processes (1) induced by almost real photons at HERA are presented and discussed. The consideration of light vector meson photoproduction is omited since this subject is covered in O.Lukina's talk [8].

[1]Units with $c = 1$ are used.

2 Soft processes

2.1 *Total hadronic photoabsorption cross section*

The total photoproduction cross section $\sigma_{tot}^{\gamma p}$ is a global characteristic of hadron physics related to the particle structure and fundamental properties of strong interactions. At the pre HERA time it was known from the fixed target experiments for energies W up to 18GeV [9].

At 10 times higher W the cross section was measured in low Q^2 ep-scattering at HERA using the tagging technique [10, 11]. Results are presented in Fig.2 together with Regge type fit of the data on $\sigma_{tot}^{\gamma p}$

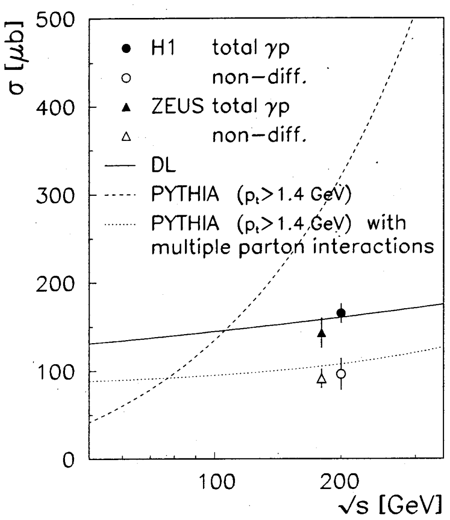

Figure 2: The total and non-diffractive cross sections for hadron photoproduction at HERA; $\sqrt{s} = W$.

at $W < 18GeV$ [12]. This fit (solid line in Fig.2) exploits the values for the intercept of the soft pomeron trajectory $\alpha_P(0) = 1.0808$ and one for the reggeon trajectory $\alpha_R(0) = 0.5475$ inferred from the data on hadrons scattering. The fit predicts the slow rise of $\sigma_{tot}^{\gamma p}$ with energy at $W > 15GeV$

$$\sigma_{tot}^{\gamma p}(W) = A \cdot W^{2\cdot(\alpha_P(0)-1)} + B \cdot W^{2\cdot(\alpha_R(0)-1)} \tag{4}$$

where $A = 67.7\mu b, B = 129\mu b$ and W in GeV. HERA results are compatible with the fit (4) and thus with prediction of VDM and the similarity in energy dependence of cross sections of photon and hadron induced reactions. The observed slow rise of $\sigma_{tot}^{\gamma p}$ is described by the soft pomeron exchange and contradicts to the prediction of mini-jets model [13] for a fast grow of the cross section at high energies (see dashed line on Fig.2).

The total photoabsorption cross section measured by H1 $\sigma_{tot}^{\gamma p} = 165.3 \pm 2.3 \pm 10.9\mu b$ [2] at $W \approx 200GeV$ [11] agrees with the ZEUS result [10] for $W \approx 180GeV$. It is worth noting that the value for the soft pomeron intercept $\alpha_P(0) = 1.11$ obtained in the study of $\bar{p}p$-interactions at c.m.s. energy $1.8TeV$ [14] would predict a stronger rise of $\sigma_{tot}^{\gamma p}$ with energy than observed at HERA.

2.2 *Diffractive and non-diffractive channels*

The decomposition of $\sigma_{tot}^{\gamma p}$ to diffractive and non-diffractive components allows for further study of soft γp physics. A nomenclature for different diffractive photoproduction processes with pomeron (**P**) exchange and for the non-diffractive process (ND) is given in Fig.3. In the elastic process (EL) a proton stays intact and according to the convention only light vector mesons (ρ, ω, ϕ) are produced; the production

[2] Here and further the first error is statistical and the second one is systematic. Given only one error means the sum in quadrature of these errors.

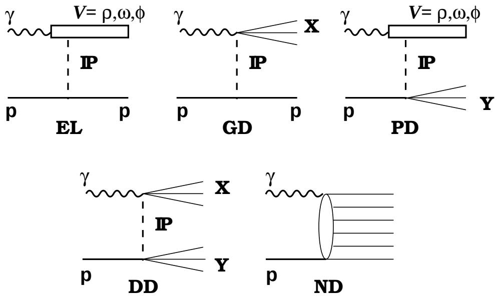

Figure 3: Diffractive and non-diffractive photoproduction processes.

of heavy vector mesons are included in the process of photon diffractive dissociation (GD). The diffractive dissociation of a target proton (PD) assumes photon conversion into ρ, ω, ϕ-mesons; in the double diffractive dissociation (DD) both the initial photon and the proton dissociate.

The total cross section can be written as

$$\sigma_{tot}^{\gamma p} = \sigma_{EL} + \sigma_{GD} + \sigma_{PD} + \sigma_{DD} + \sigma_{ND}. \tag{5}$$

Owing to the different event topology of diverse photoproduction processes it is possible to measure the cross sections of EL, GD and PD processes assuming a reasonable value for $\sigma_{DD} = 15\mu b$. The results of the H1 measurement [11] and comparison with the theoretical expectations of Regge inspired models [15, 16, 17] are given in the Table 1.

Table 1. The cross sections in μb for diffractive processes (Fig.3) at $W = 200GeV$.

PROCESS	EL	GD	PD	DD
DATA [11]	17±4	26±5	9±2	15 assumed
CKMT [15]	17	25	7	15
SaS [16]	16	13	10	13
GLM [17]	17	18	15	15

These H1 results are in agreement with earlier obtained by ZEUS [10] (at lower energy: $W = 187GeV$) $\sigma_{EL} = (18 \pm 7)\mu b$ and $\sigma_{GD} + \sigma_{PD} + \sigma_{DD} = (33 \pm 8)\mu b$. It should be mentioned that both experiments gave a rather big value ($\approx 40\%$) for the portion of diffractive contribution to $\sigma_{tot}^{\gamma p}$ in comparison with hadron processes. As is seen from Table 1 a better description of the data is obtained in the model [15] where the absorptive corrections to soft diffractive processes are taken into account. The accuracy of the cross sections measurements for EL and GD processes was improved in a recent H1 study [18]: $\sigma_{EL} = (18.2 \pm 0.8 \pm 2.8)\mu b$ and $\sigma_{GD} = (21.5 \pm 0.6 \pm 5.9)\mu b$.

The main contribution to σ_{EL} is given by ρ^0-meson photoproduction. The energy dependence of the cross section $\sigma(\gamma p \to \rho^0 p)$ is consistent with soft pomeron exchange [8]

$$\sigma(\gamma p \to \rho^0 p) \propto \frac{W^{4(\alpha_P(0)-1)}}{b}. \tag{6}$$

Here the slope parameter b of the diffraction cone grows logarithmically with the energy. To good approximation the expression (6) can be rewritten as $\sigma \propto W^\delta$ with $\delta \approx 0.22$.

The important feature of soft diffractive physics is the dependence of the GD cross section on the mass M_X of the state to which the photon dissociates. The triple pomeron amplitude approach predicts $d\sigma/dM_X^2 \propto (1/M_X^2)^{\alpha_P(0)}$ for high M_X. The prediction was checked in [18, 19]. The H1 investigation [18] was performed at energy $W = 187GeV$ in the wide range of mass $1.0GeV^2 < M_X^2 < 500GeV^2$. The fit to these data (solid line on Fig.4) in the form $d\sigma/dM_X^2 \propto (1/M_X^2)^n$ led to $n = 1.03 \pm 0.02 \pm 0.07$

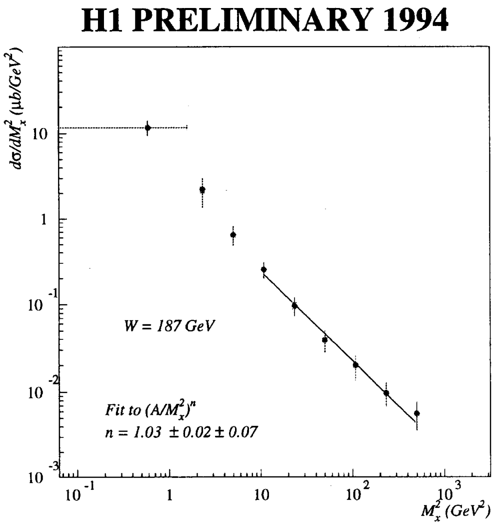

Figure 4: The dependence of the photon dissociation cross section (process GD) on M_X^2 and fit to it.

for $M_X^2 > 10GeV^2$ in close agreement with expectations $n = \alpha_P(0)$. The ZEUS investigation [19] at $W \approx 200GeV$ gave similar result: $n = 1.14 \pm 0.04 \pm 0.08$.

Just as in soft hadronic reactions, a rapid, approximately exponential, decrease of the p_T [3] spectra for inclusive charge particle production is observed in soft diffractive and non-diffractive photon induced processes at HERA [20] (Fig.5). For soft processes ($p_T \leq 1GeV$) this decrease can be described in the

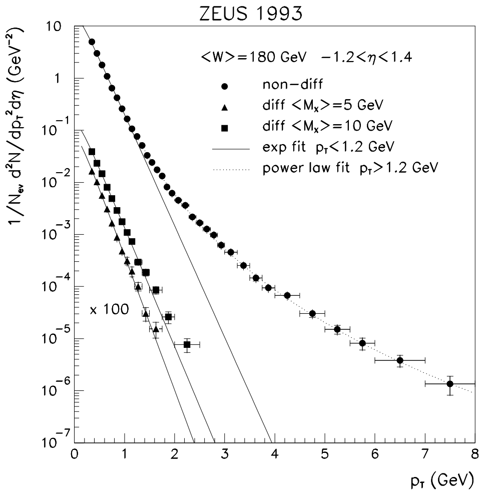

Figure 5: Charge particle distributions *vs* transverse momentum p_T in GD and ND processes at $W = 180GeV$ for $-1.2 < \eta < 1.4$.

thermodynamic model [21]

$$\frac{1}{N} \cdot \frac{d^2N}{dp_T^2 d\eta} \sim \exp\left(a - b\sqrt{p_T^2 + m_\pi}\right) \tag{7}$$

where m_π is the pion mass. The fit of the measured distributions for $p_T < 1.2GeV$ (the solid lines in Fig.5) gave for the parameter b which characterizes the exponential fall for small p_T the values $b_{ND} = (4.94 \pm 0.09 \pm 0.9)GeV^{-1}$ for non-diffractive process and $b_{GD} = (5.91 \pm 0.17 \pm 0.19)GeV^{-1}$ for diffractive photon

[3] p_T is hadron transverse momentum.

dissociation with $M_X^2 = 5GeV^2$. These values are close to the results obtained in hadron interaction experiments.

The results of the measurements of σ_{ND} are given in Fig.2. A Monte Carlo (MC) algorithmical approach PYTHIA [22] which incorporates the physics of soft and hard interactions for photon induced reactions predicts for the transverse momentum of parton $p_t > p_t^{min} = 1.4GeV$ a rather sharp rise of σ_{ND} with energy (similar to the prediction of the mini-jet model [13]) shown in Fig.2 by the dashed curve. But after taking into account multiple parton interactions and applying a unitarization procedure [23] the calculated σ_{ND} is consistent with the data (dotted line in Fig.2).

As is seen in Fig.5 the particle p_T spectra in diffractive processes fall exponentially with p_T rise whereas non-diffractive distribution flattens at $p_T > 1.2GeV$. This is a sign of the partonic structure of the interacting particles and of the transition to the regime of hard scattering described by perturbative QCD.

3 Hard Photoproduction

3.1 *Inclusive spectra*

At high p_T ($> 1GeV$) the non-diffractive contribution to inclusive spectrum of reaction (1) becomes dominant (Fig.4) and its decrease follows the prediction of a QCD power law [21]:

$$\frac{1}{N} \cdot \frac{d^2N}{dp_T^2 d\eta} \sim (1 + \frac{p_T}{p_{T_0}})^{-n}. \tag{8}$$

The fit of H1 data [24] for energy $W = 200GeV$ in the pseudo-rapidity and p_T intervals $|\eta| < 1.5$ and $1.5GeV < p_T < 8GeV$ gave $n = 7.1 \pm 2.0$ and $p_{T_0} = 0.63 \pm 0.20GeV$. These values are compatible with the more recent ZEUS data [20] for $W = 180GeV$ in approximately the same η and p_T intervals: $n = 7.25$ and $p_{T_0} = 0.54GeV$.

The comparison of measured inclusive spectra of charged particles in photon and hadron induced reaction at different energies shows (Fig.6) that normalized to corresponding total cross sections

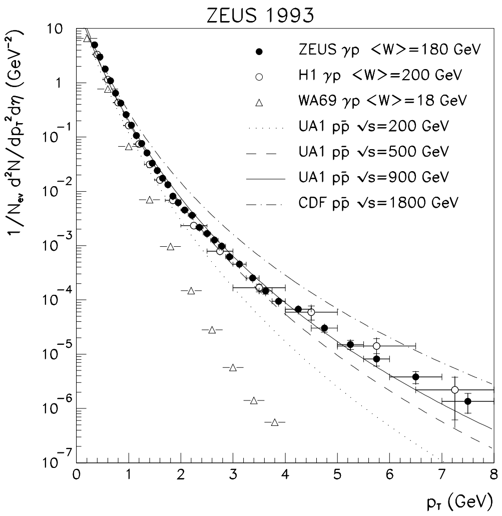

Figure 6: High p_T charge particle spectra measured in γp and $p\bar{p}$-interactions for different c.m.s. energies.

1) the data of ZEUS [20] and H1 [24] are in agreement with each other,
2) the photoproduction spectra for low W ($W = 18GeV$ [25]) are softer than for HERA energies,
3) p_T distributions in photoreactions are harder than in the $\bar{p}p$ interactions at the corresponding energy. The last point is illustrated by fitting the $\bar{p}p$ data on inclusive spectra at c.m.s. energy $200GeV$ [26]

with the result $n = 12.14 \pm 0.39$ and $p_{T_0} = (1.8 \pm 0.1) GeV$. This is connected with the existence of an additional mechanism in γp-interactions in comparison with hadron interactions.

In Leading Order (LO) QCD the hard photoproduction is characterized by *resolved* and *direct* interactions (Fig.7). The *resolved* part contains VDM contributions which are responsible for the similarity of

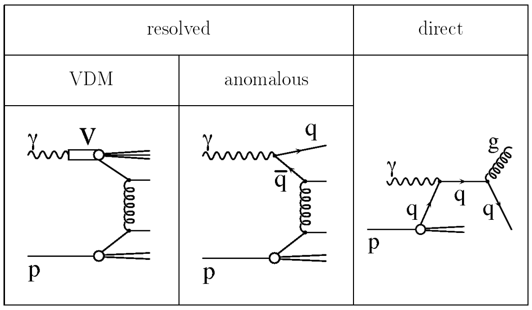

Figure 7: Examples of LO QCD diagrams for resolved and direct photoproduction processes.

hadron and photon induced processes and by the contribution to the γp amplitude of the so called *anomalous* component [27], corresponding to the coupling of the photon with a free $q\bar{q}$-pair. In *direct* interactions the photon couples directly with partons in the nucleon through QCD Compton and photon-gluon fusion (PGF). The *direct* and the *anomalous* parts which play an essential role at high p_T^2 ($> 50 GeV^2$) are responsible for peculiarities of photon-hadron interactions. But overall the photoproduction of light quarks is governed by the *resolved* process.

The absolute values of the inclusive differential cross sections $d^2\sigma/dp_T^2 d\eta$ measured by H1 [24] and ZEUS [20] for $p_T > 1.5 GeV$ are successfully described by the analytical calculations in Next to Leading Order (NLO) QCD [28] performed with the use of photon [29] and proton [30] structure functions. It should be mentioned that in NLO QCD there is no simple division for *direct* and *resolved* components as in LO.

Important information on the parton dynamics of photoproduction can be obtained from the events with large transverse energy E_T. Results of recent measurements of the low Q^2 ep-scattering cross section $d\sigma/dE_T$ and energy flow $dE_T/d\eta^*$ [31] for $20 GeV < E_T < 50 GeV$ and $-2.5 < \eta^* < 1$ (η^* is pseudorapidity in the γp c.m.s.) are given in Fig.8 where the comparisons of the data with MC PYTHIA [22] and PHOJET [32] are provided. Both MC use Lund fragmentation scheme JETSET [22] for the parton hadronization process and include parton showering in initial and final states. Multiple parton scattering can play an essential role in the process of hard photoproduction. It is seen that MC PYTHIA without implementation of multiple parton rescattering (dotted lines in Fig.8a) does not describe the measured $d\sigma/dE_T$. Taking into account these corrections (PYTHIA-mia) improves the situation (dashed line) but there is still some discrepancy at $E_T < 30 GeV$. More satisfactory agreement with data is reached with MC PHOJET (full line), which includes the parton rescattering corrections from the very beginning. PHOJET and PYTHIA-mia give a reasonable description of the measured $dE_T/d\eta^*$ for $25 GeV < E_T < 30 GeV$ whereas PYTHIA without rescattering corrections does not agree with the data (Fig.8b). Thus study of these corrections (which plays a decisive role also in getting a satisfactory description of data on $\sigma_{tot}^{\gamma p}$ - see Fig.2) clarifies the parton dynamics of hard photoproduction process.

3.2 *Jet Photoproduction*

The underlying parton picture of hard photon induced processes (Fig.7) leads to the jet topology of photoproduction events. In the *direct* processes two high momentum transverse jets balancing each other are expected as a result of fragmentation of the current partons; the parton-spectator develops to the proton remnant jet which has low transverse energy and therefore disappears as a rule in the beam pipe. The *resolved* process contains also the second remnant jet - from the photon constituent. MC simulation shows clearly the correlation between jets and partons and thus jet distribution investigations shed light on a parton interaction picture.

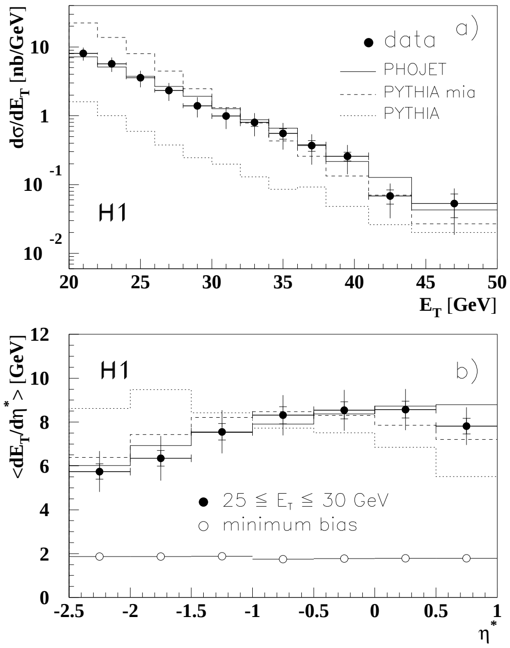

Figure 8: Measured transverse energy distribution $d\sigma/dE_T$ and energy flow $dE_T/d\eta^*$ together with MC predictions.

H1 [31] and ZEUS [33] investigations of jet photoproduction process were performed for jet transverse energies $E_T^{jet} > 6GeV$ in the jet pseudo-rapidity interval $-1 < \eta^{jet} < 2$. For jet identification the cone jet finding algorithm [34] was used with the cone radius $R = 1$. It is natural to expect that jets become more pronounced with the rise of their energy (and hence E_T^{jet}). The experiment shows that the observed jet multiplicity are growing with visible transverse energy (E_T^{vis}) in the calorimeter (Fig.9) in the studied transverse energy interval from $25GeV$ to $40GeV$. MC calculations taking into account parton multiple

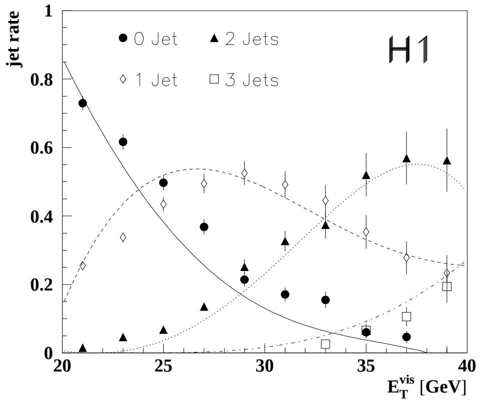

Figure 9: Jet rate *vs* the visible transverse energy E_T^{vis}.

scattering (the curves in Fig.9) satisfactory describe the observed jet rates. It should be stressed that at $E_T^{vis} > 35GeV$ there are almost no events without jets and the rate of three jet events arising from the higher order QCD processes or from the *resolved* reaction are greater than 10%.

The angular spread of jets (its width Γ) measured in the photoproduction process goes down with the rise of E_T^{jet} in accordance with the QCD prediction and with the observations in other hard processes ($\bar{p}p$ interactions, e^+e^- annihilation). This demonstrates the universality of jets properties. The width $\Gamma(rad)$ is successfully fitted by the dependence $\Gamma(rad) \sim 1/E_T^{jet}$ [23].

The analysis of the hadron final state in photon induced reactions using the jet finding cone algorithm gave the possibility to measure absolute values of jet the production cross section. The low-Q^2 electroproduction cross sections $d\sigma/dE_T^{jet}$ and $d\sigma/\eta^{jet}$ obtained for $-1 < \eta^{jet} < 2$ and $7GeV < E_T^{jet} < 30GeV$ by ZEUS [33] and H1 [31] are in the agreement with each other. The E_T^{jet} dependence of the differential cross section is characterized by the power law $d\sigma/dE_T^{jet} \propto (E_T^{jet})^{-n}$ with $n = 6.1 \pm 0.5$ [31]. This value is close to $n = 5.8$ obtained in the study of $\bar{p}p$ interactions [35]. Fig.10 shows the η^{jet} distributions [33] integrated over E_T^{jet} from thresholds $8, 11, 17GeV$ to maximal E_T. It is seen that $d\sigma/d\eta^{jet}$ rises with

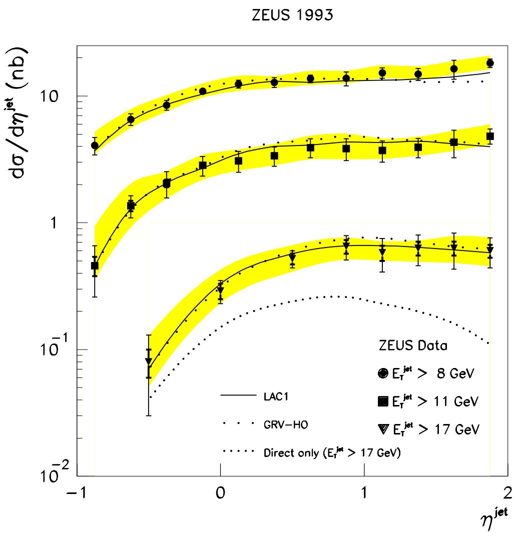

Figure 10: The inclusive cross section $d\sigma/\eta^{jet}$ for low Q^2 electroproduction of jets with E_T^{jet} above 8, 11 and $17GeV$.

pseudo-rapidity in the low η region. The only *direct* photoproduction mechanism (dotted curve in Fig.10) does not describe the data. MC PYTHIA calculations with *direct* and *resolved* contributions and LAC1 [36] or GRV-HO [37] photon structure functions are in reasonable agreement with these data. The shaded area in Fig.10 indicates uncertainty due to the energy scale of jets. The H1 study [31] shows that the better description of measured $d\sigma/dE_T^{jet}$ and $d\sigma/d\eta^{jet}$ is provided by MC PHOJET.

3.3 *Direct and Resolved Photoproduction*

The separate study of *direct* and *resolved* components in hard photoproduction is of great importance since it gives the information on special properties of γp-interactions, on the parton distributions in the proton and the photon.

In the *resolved* process spectator partons in the photon and proton fragment into two low p_T jets moving close to the collision axis. Because of the boost of γp c.m.s. in the direction of the initial proton at HERA the photon remnant jet can emerge at noticeable angle in the backward direction to be detected. The search for the lowest p_T backward jets in three jet photoproduction events led to the observation [38] of the photon remnant jet from the *resolved* process. Two jets from parton-parton interaction in *resolved* process had $p_T > 6GeV$ whereas the photon remnant jet had $< p_T >= 2.1 \pm 0.2GeV$ and arose at $\eta < -1$. To identify jets with so low p_T the $k_\perp$ clustering algorithm [39] was used. Thus the photon remnant has jet like behavior and its substantial $< p_T >$ value demonstrate rather hard distribution of partons in a photon.

The way to separate the *direct* and *resolved* contributions is the study of event distribution *vs* x_γ which is the fraction of photon momenta carried by the interacting parton in a γ. For the *direct* process x_γ is equal to 1 and events with $x_\gamma < 1$ are due to *resolved* photoproduction. The distribution can be measured in high E_T^{jet} dijet photoproduction but because of parton hadronization effects x_γ is modified to x_γ^{OBS} which is slightly smeared and shifted to lower values relative x_γ. x_γ^{OBS} is expressed through the transverse energies of these 2 jets and corresponding pseudo-rapidities as follows

$$x_\gamma^{OBS} = \frac{E_T^{jet1} \cdot \exp(-\eta^{jet1}) + E_T^{jet2} \exp(-\eta^{jet2})}{2E_\gamma}. \tag{9}$$

In the ZEUS studies [40, 41] jets with $E_T^{jet} > 6GeV$ and $-1.37 < \eta^{jet} < 1.87$ were identified using the cone and $k_\perp$ clustering algorithms. Differential cross sections $d\sigma/d\bar{\eta}$ where $\bar{\eta} = (\eta^{jet1} + \eta^{jet2})/2$ were measured for jet rapidities difference $\Delta\eta = \eta^{jet1} - \eta^{jet2} < 0.5$. The obtained dijet event distribution *vs* x_γ^{OBS} (Fig.11) has the peaks corresponding to the *direct* ($x_\gamma^{OBS} > 0.75$) and *resolved* ($x_\gamma^{OBS} < 0.75$) mechanisms of photoproduction. MC simulation of *direct* processes within the program HERWIG [42]

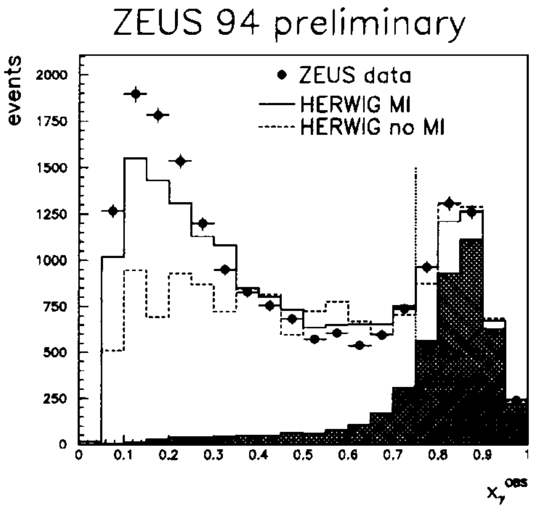

Figure 11: Dijet events distribution in x_γ^{OBS}.

gives a rather good description of the data at $x_\gamma^{OBS} > 0.8$ (shaded area in Fig.11). At $x_\gamma^{OBS} < 0.3$ the MC curves normalized to the data at $x_\gamma^{OBS} > 0.3$ (dashed histogram) lie below the experimental points. Taking into account multiple parton interactions (HERWIG MI) improves the data description (full histogram) but not completely. The measured *direct* cross section is in a good agreement with NLO QCD calculations. However the cross section of the *resolved* process is a factor of two less than these calculations predict.

It is possible to check how good is such isolation of the *direct* and *resolved* components using the fact that the main contribution to the *direct* processes is given by PGF with a quark exchange in the t-channel (spin 1/2 particle) whereas the *resolved* reactions are mainly due to quark or gluon scattering subprocesses via a gluon exchange (spin 1 particle). Examples of relevant diagrams are given in Fig.12. The angular distribution of two current jets in their c.m.s. is given by (θ^* is the angle between jets axis and photon beam direction)

$$\propto \frac{1}{(1 - |\cos\theta^*|)^2} \tag{10}$$

for the case of spin 1 exchange particle (gluon) in *resolved* process and by

$$\propto \frac{1}{(1 - |\cos\theta^*|)} \tag{11}$$

for the exchange of spin 1/2 particle (quark) in *direct* process. These distributions are quite different especially for small $|\theta^*|$ and should be distinguishable in the experiment.

The ZEUS study [43] of the photoproduction of two jets with $E_T^{jet} > 6GeV$, dijet invariant mass $M_{jj} > 23GeV$ and average pseudo-rapidity $\bar{\eta} < 0.5$ gave different angular distributions for $x_\gamma^{OBS} < 0.75$

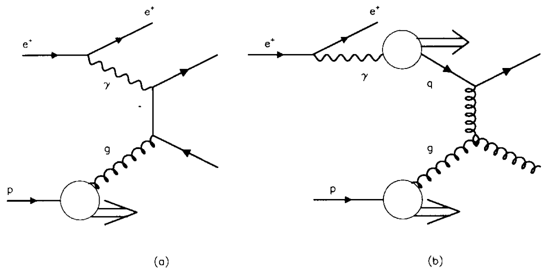

Figure 12: Diagrams of the main contributions to the *direct* (a) and the *resolved* (b) photoproduction.

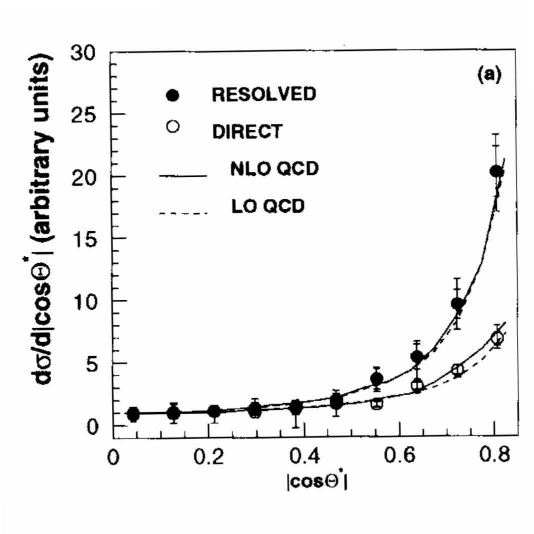

Figure 13: The dijet cross section $d\sigma/d|\cos\theta^*|$ normalized to 1 at $\cos\theta^* = 0$ for *direct* and *resolved* photoproduction.

and > 0.75 (Fig.13). The measured cross sections $d\sigma/d|cos\theta^*|$ for *resolved* and *direct* processes are compatible with expectations (10) and (11) respectively. MC PYTHIA and HERWIG give satisfactory descriptions of these angular distributions. The predictions of NLO and LO QCD (solid and dashed curves on Fig.13) are close to each other and also agree with these experimental distributions.

The H1 study [44] of dijet photoproduction process for $E_T^{jet} > 7GeV$ and $0 < \eta^{jet} < 2.5$ allowed to extract the gluon distribution in a photon $g(x_\gamma)$. It is especially interesting since the investigation of deep inelastic $e\gamma$-collisions at e^+e^--colliders provides the information mainly on quark content of the photon [45]. In the measurement [44] x_γ was determined from two highest E_T jets using the jet-parton correlation. The obtained event distribution in x_γ shows the excess at $x_\gamma < 0.2$ over the expected number of events if only the quark contribution to photon structure function is taken into account. By subtraction of the calculated quark contribution from the observed number of events and by the interpretation of the rest in term of the gluon contribution the $x_\gamma \cdot g(x_\gamma)$ was obtained. In the calculations GRV-LO fit of the quark distribution in the proton [46] was used. The measured in such a way the gluon density in the photon (Fig.14) is compatible with GRV-LO fit [37] (solid curve) and does not agree with LAC1 (dashed curve) and LAC3 (dotted curve) parametrizations [36].

Experimental evidence for the *anomalous* component of *resolved* γp-interaction was obtained in the H1 investigation [47] where the production of two jets with $E_T^{jet} > 8GeV$, $-0.5 < \eta^{jet} < 2.5$ and rapidities difference $\Delta\eta < 1$ were investigated. The cone finding algorithm with radius $R = 0.7$ was used to identify jets.

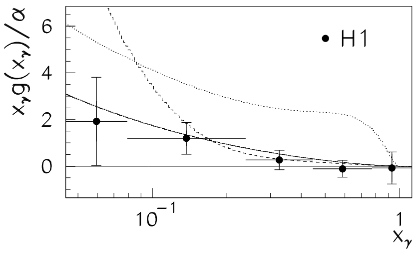

Figure 14: The gluon density in a photon $g(x_\gamma)$. α is the fine structure constant.

The effective parton distribution in the photon $f_{i/\gamma}$ can be presented in a form [48]

$$f_{i/\gamma} = \Sigma(q + \bar{q}) + 9/4 \cdot g, \tag{12}$$

where $q(x_\gamma)$ and $\bar{q}(x_\gamma)$ are quark and antiquark densities. Inferred from the data [47] differential dijet cross section $d^2\sigma/dx_\gamma^{jet} d\log(E_T^2/E_0^2)$ ($E_0 = 1GeV$, E_T is transverse energy of the second highest E_T^{jet} jet) is described satisfactory by PYTHIA-mia and GRV-LO parton distributions in the proton [46] and the photon [37]. This cross section was transformed using the jet-parton correlation to the parton cross section $d^2\sigma/dx_\gamma d\log p_t^2$ from which the effective parton distribution in a photon $f_{i/\gamma}$ was extracted for $0.1 < x_\gamma < 0.75$. Results are given in Fig.15 where the dependence of $x_\gamma \cdot f_{i/\gamma}/\alpha$ on transverse parton

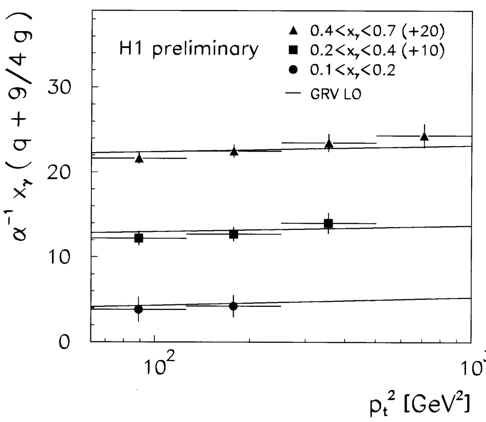

Figure 15: The effective parton distribution (12) in a photon. Solid curves are GRV-LO fit.

momentum p_t^2 for different x_γ is shown. The observed slow rise of $f_{i/\gamma}$ with p_t^2 is in agreement with the expectation from the *anomalous* contribution [27]. In the region $0.4 < x_\gamma < 0.7$ where the contribution of the gluon content of the photon to the effective parton density is only 20% the rise is due mainly to $\bar{q}q$ content of the photon.

3.4 *Hard Diffraction in γp-interactions*

The photon diffractive dissociation process (GD on Fig.3) which is characterized by an exchange of a pomeron (colourless object with vacuum quantum numbers) led at HERA to a gap in rapidity distribution of final hadrons in the direction adjoined to the proton beam.

Measured by H1 [49] photoproduction events distribution in the η_{max} (η_{max} is the pseudo-rapidity for the most forward hadron) shows a shoulder at $\eta_{max} < 1.5$ (Fig.16) corresponding to rapidity gap (RG) events. The shoulder is described satisfactory by MC PYTHIA option which includes single diffraction (sd=GD+PD) processes (full curve in Fig.16). The non diffractive (nd) component of γp-interaction gives the main contribution at $\eta_{max} > 2$ and dies exponentially at $\eta_{max} < 2$ (shaded area in Fig.16). The sum of sd and nd component (full curve) satisfactory describe the data.

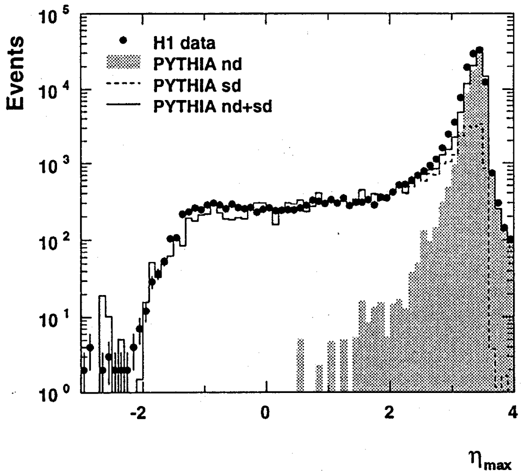

Figure 16: Events distribution *vs* η_{max} in photoproduction.

The measurement of particle p_T spectra for $-1.5 < \eta < 1.5$ in these RG events revealed [49] a long tail at high p_T which is specific for hard processes (Fig.17). It is seen that the model of soft diffraction (dot-dashed histogram) disagrees with the data at $p_T > 1GeV$ while POMPYT [50] which takes into account hard diffraction gives reasonable description of the data (full histogram in Fig.17 is a sum of soft and hard diffractive components). A similar conclusion was obtained from the study of transverse energy E_T distribution (for $E_T > 5GeV$ and $\eta_{max} < 1.5$) in ZEUS study [51]. It was also shown there that the rate of hard RG events did not fall down with the rise of energy W which is typical for pomeron exchange processes and in agreement with MC POMPYT predictions. The thrust analysis of RG events in H1

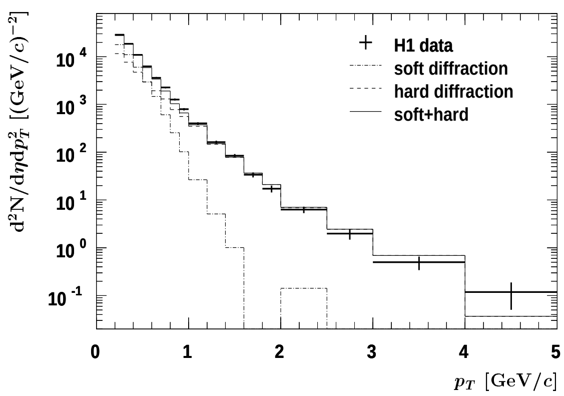

Figure 17: Charge particle p_T distribution in RG events.

data [49] reveals an azimuthal back-to-back correlation of transverse energy flow at large E_T ($> 9GeV$) what is specific for the hard processes of jet production.

Jets in RG photoproduction events were observed [49, 51] and studied in detail in [51, 52]. The core structure of these jets is the same as for those observed in the standard hard photoproduction. The fraction of RG events with jet production is growing with E_T and at $E_T > 12GeV$ the majority of events has 2 or more jets [51]. It is interesting to note that x_γ distribution of RG events obtained from the two jet data sample has a maximum at $x_\gamma \approx 1$ [51] and hence shows a large contribution of *direct* photoproduction in hard diffraction. The recent ZEUS study [53] gave also evidence for the contribution of *resolved* processes at $x_\gamma < 0.8$ which is successfully described by MC POMPYT.

Thus hard photoproduction in the RG events has the features of diffractive processes. They can be understood in terms of the exchange of hard pomeron having a partonic structure [54]. There are several models for the parton density distributions in a pomeron $f_{p/\mathbf{P}}$:

a superhard gluon density

$$\beta \cdot f_{g/\mathbf{P}} = 0.1/(1-\beta)^{0.9}, \tag{13}$$

a hard gluon density

$$\beta \cdot f_{g/\mathbf{P}} = 6\beta(1-\beta), \tag{14}$$

a soft gluon density

$$\beta \cdot f_{g/\mathbf{P}} = 6(1-\beta)^5, \tag{15}$$

and a hard quark density

$$\beta \cdot f_{q/\mathbf{P}} = 6\beta(1-\beta)/4. \tag{16}$$

Here β is a fraction of the pomeron momentum carried by parton in the pomeron. MC POMPYT predictions for these models were obtained with the use of pomeron flux factor from the paper [54]. The inclusive cross section of jet photoproduction process $d\sigma/d\eta^{jet}$ measured for $E_T^{jet} > 8GeV$ and $-1.5 < \eta < 1.5$ [52, 53] is compared with the predictions on Fig.18 where the shaded area reflects the uncertainty in the jet energy scale. The experimental data gave an evidence in favour of hard (or

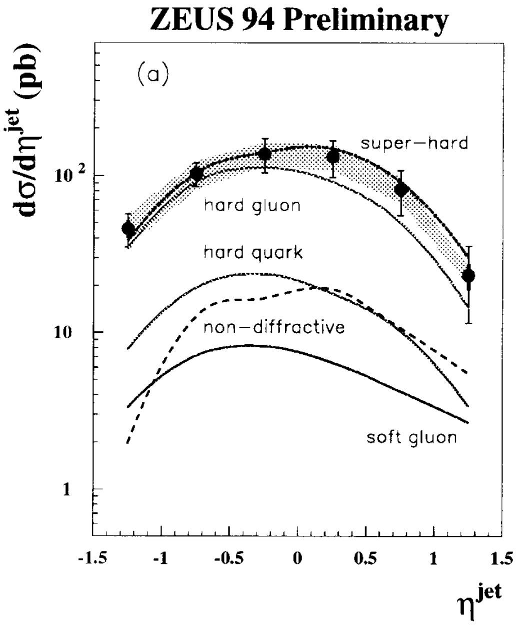

Figure 18: Inclusive cross section $d\sigma/d\eta^{jet}$ in RG events together with the expectations from different quark and gluon distributions (13-16) in a pomeron.

superhard) gluon density in the pomeron. The non-diffractive model of the hard photoproduction (MC PYTHIA, the dashed curve) does not agree with these data. Soft gluon distribution in $\mathbf{P}$ and hard quark content of pomeron also are not compatible with experimental cross section $d\sigma/d\eta^{jet}$.

The measured in ZEUS study [53] $d\sigma/dE_T^{jet}$ for $\eta^{max} < 1.8$ falls down exponentially with the rise of E_T^{jet} in agreement with hard gluon distribution in the pomeron. The measured M_X spectrum of final hadronic system in RG hard photoproduction events is also compatible with diffractive reaction mechanism and with the results of MC POMPYT calculations for the hard gluon density.

The exchange of colourless objects can also take place between current partons in jet photoproduction reactions (Fig.19). In the case of pomeron exchange a number of events with rapidity gap between two jets (without hadron activity in a corresponding $\Delta\eta$ which is a pseudo-rapidity distance between jets axes) should exist. An estimation of the fraction of such events in the hard processes by modeling of colourless object as two gluons colour singlet state and the standard hard interaction as one gluon exchange [55] gives the value of $\approx 10\%$. To reveal this phenomenon in photoproduction process dijet events with $E_T^{jet} > 6GeV$, $\eta^{jet} < 2.5$, $\Delta\eta > 2$ and $\bar{\eta} =< 0.75$ were investigated at ZEUS detector [56]. It is expected

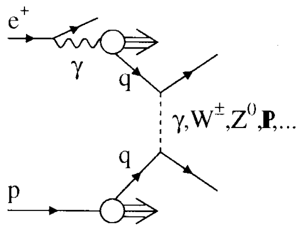

Figure 19: The example of colour singlet exchanges between current partons in a resolved photoproduction.

that the gap-fraction $f(\Delta\eta)$ which is defined as a fraction of the number of rapidity gap events within this interval $\Delta\eta$ to the total number of dijet events in the same interval will decrease with $\Delta\eta$ increasing for colour non-singlet exchange and will be almost independent of $\Delta\eta$ for colourless exchange [55]. The measured gap-fraction is shown in Fig.20. It is seen that the dependence $f(\Delta\eta)$ is characterized by the

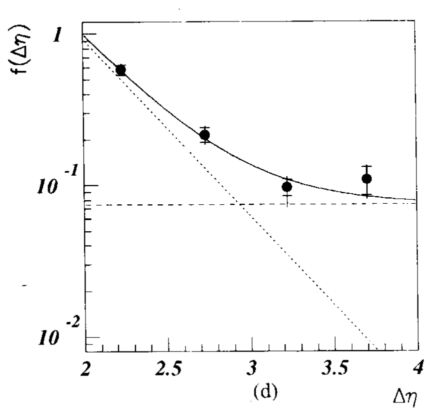

Figure 20: The gap-fraction $f(\Delta\eta)$ *vs* the pseudo-rapidity interval between jets axes.

exponential fall for $\Delta\eta < 3$ and by the constant term at larger $\Delta\eta$. In the fit to the data (solid curve in Fig.20) the exponential part (dotted line) is in agreement with the standard MC PYTHIA which does not take into account colourless exchange between jets. The constant term (dashed curve) has the value $0.07 \pm 0.02^{+0.01}_{-0.02}$ which is close to QCD estimation [55]. It is evidence for a diffractive interaction between current partons. Similar observation was made in the study of jet production in $\bar{p}p$-interactions [57, 58] but with an approximately order of magnitude smaller effect.

4 Heavy Flavour (Charm) Production

4.1 *Charmonium*

Rather high masses of ψ-mesons ($\geq 3.1 GeV$) provide the conditions for considering their photoproduction as QCD hard process although the VDM approach [1] together with the Reggeon phenomenology [12, 59] is also used in the discussion of the data.

In the fixed target experiments the photoproduction of J/ψ-mesons was studied at $W < 30GeV$. At HERA these studies were extended to energies $30 < W < 260GeV$. J/ψ particles were detected through their decay to lepton pair (e^+e^- or $\mu^+\mu^-$) with a clear signal [60, 61] (narrow peak in the mass distribution of dilepton pair at $\approx 3.1GeV$). Possible production mechanisms are presented in Fig.21.

The elastic process

$$\gamma + p \to J/\psi + p \tag{17}$$

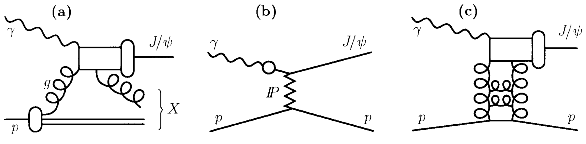

Figure 21: Diagrams of inelastic (a) and elastic (b,c) J/ψ photoproduction on a proton.

can proceed through pomeron or ladder gluon exchange. In the inelastic process

$$\gamma + p \rightarrow J/\psi + X \tag{18}$$

final state hadrons arise as a result of the proton diffractive dissociation (process PD in Fig.3 with V=J/ψ) or photon gluon fusion (PGF).

The event topology in detectors for charmonium photoproduction is used to distinguish elastic, proton diffractive dissociation and inelastic processes. To select the elastic process no activity in the detector is required apart from the observation of the dilepton pair from J/ψ decay. Further, the cut in the data on the elasticity parameter $z = E'_{J/\psi}/E'_\gamma > 0.95$ (here E' are energies in the proton rest system) helped to separate elastic events. The results of cross section measurements for elastic process [62, 63] is shown in Fig.22 together with fixed target data. The data show a sharp rise of $\sigma(\gamma p \rightarrow J/\psi p)$ with

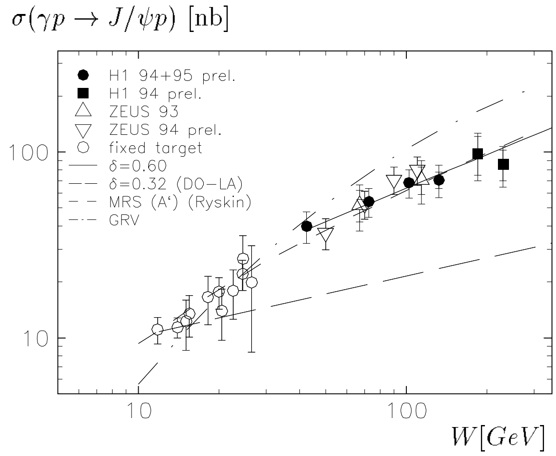

Figure 22: The cross sections $\sigma(\gamma p \rightarrow J/\psi p)$ measured at HERA and in fixed target experiments ($W < 30GeV$).

the energy W. The power fit $\sigma_{el} \sim W^\delta$ of HERA data gives $\delta = 0.60 \pm 0.12$ (solid line in Fig.22). This is in strong contradiction with the soft pomeron exchange model [12, 59] which predicts according to (6) $\delta = 0.22 - 0.32$ (long dashed line normalized to the fixed target data) but in line with the hard pomeron concept with intercept $\alpha_P(0) \approx 1.2$ ($\delta \approx 0.8$, see *e.g.* [64]). The ladder gluon exchange model [65] (diagram c in Fig.21) and its NLO QCD modification [66] gives a reasonable description of the data (dashed curve) when the MRS(A') parametrization of the gluon distribution in the proton [67] is used. It is interesting to note that in this model the cross section is proportional to the square of the gluon density in the proton and therefore is sensitive to its form. The use of the GRV parametrization [29] for it instead of MRS(A') gives a different prediction for $\sigma(\gamma p \rightarrow J/\psi p)$ (the dot-dashed curve on Fig.22).

The $p^2_{TJ/\psi}$ dependence of differential cross section of the elastic process ($p_{TJ/\psi}$ is the transverse momentum of J/ψ-meson) was measured for $p^2_{TJ/\psi}$ up to $2GeV^2$ at energies $30 < W < 150GeV$. The exponential fit to the data $d\sigma/dp^2_{TJ/\psi} \propto A \cdot \exp(-bp^2_{TJ/\psi})$ for $p^2_{TJ/\psi} < 1GeV^2$ gave the result: $b^{J/\psi}_{el} = (4.1 \pm 0.2 \pm 0.2)GeV^{-2}$.

The cross section of J/ψ photoproduction with diffractive dissociation of the proton (PD) can reach $\approx 50\%$ of $\sigma(\gamma p \rightarrow J/\psi p)$ according to H1 measurements [68]. PD events were selected by the requirement to have some activity in the forward subdetectors. The fit to the energy dependence of this cross section in the form $\sigma \propto W^{\delta}$ gave $\delta = 1.2 \pm 0.2$. The differential cross section $d\sigma/dp^2_{T\,J/\psi}$ has a smaller slope than one for the elastic photoproduction: $b^{J/\psi}_{PD} = (1.6 \pm 0.3 \pm 0.1)GeV^{-2}$.

The measured angular distributions of dilepton pairs from J/ψ decay are consistent with helicity conservation in elastic and PD photoproduction processes [62, 68] at HERA energies. This property and exponential fall off $d\sigma/dp^2_{T\,J/\psi}$ are the specific features of diffractive nature of the process.

Inelastic J/ψ photoproduction was studied by means of the selection of events with $z < 0.8$. The measured cross section of the process (18) for $p^2_{T\,J/psi} > 1GeV^2$ is shown in Fig.23. The cross section

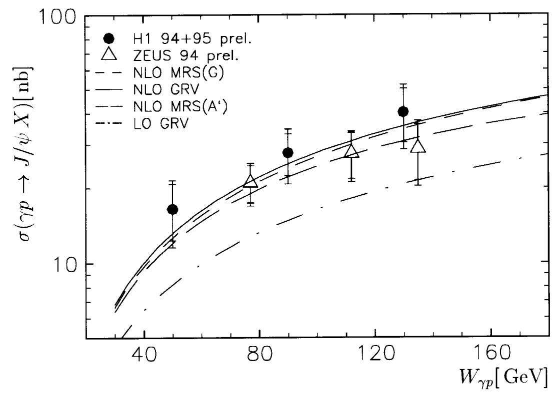

Figure 23: The measured at HERA cross section for inelastic J/ψ photoproduction.

grows with W but not so drastically as for the elastic process. The obtained $\sigma(\gamma p \to J/\psi X)$ exceeds predictions of LO colour singlet model [69] (dash-dotted curve). Taking into account NLO terms [70, 71] brings the theory predictions for charm quark mass $m_c = 1.5GeV$ and the scale parameter $\Lambda = 300MeV$ into agreement with the experimental data irrespective of the gluon distribution in the proton which is chosen in the calculations (the solid curve in Fig.23 corresponds to the structure function [29]).

The differential cross section of inelastic photoproduction shows also a weaker dependence on $p^2_{T\,J/\psi}$ than the cross sections of elastic and PD processes. NLO QCD predictions agree with the data in the restricted kinematics region ($z < 0.8$ and $p^2_{T\,J/\psi} > 1GeV^2$) where theoretical calculations are applicable. The exponential fit $d\sigma/dp^2_{T\,J/\psi}(\gamma p \to J/\psi X) \propto \exp(-b_{in} p^2_{T\,J/\psi})$ to H1 data [68] in the region $z < 0.9$ and $1GeV^2 < p^2_{T\,J/\psi} < 5GeV^2$ gives $b^{J/\psi}_{in} = (0.39 \pm 0.06 \pm 0.03)GeV^{-2}$ in close agreement with NLO prediction $0.3GeV^{-2}$ [71]. The NLO calculations in the colour singlet model also give a good description of the measured differential energy distribution $d\sigma/dz$.

The photoproduction of $\psi'(2S)$-meson with the mass $\approx 3.7GeV$ was studied at HERA at the energy $W \approx 80GeV$ [68, 72]. ψ' was detected in 4 prong events ($\pi^+\pi^-l^+l^-$) which arise as a result of the decay $\psi' \to J/\psi\pi^+\pi^-$ and a subsequent J/ψ decay to a lepton pair. The cross section was measured for the elasticity parameter $z > 0.95$ where diffractive processes (elastic and proton dissociation) are dominant: $\sigma^{diff}(\gamma p \to \psi'(2S)X) = (19 \pm 5 \pm 4)nb$. It was found that the ratio

$$\frac{\sigma^{diff}(\gamma p \to \psi'(2S)X)}{\sigma^{diff}(\gamma p \to J/\psi X)} = 0.16 \pm 0.06 \qquad (19)$$

is close to this value at low energies ($W < 20GeV$) (see for example [73]) *i.e.* does not depend strongly on the energy.

4.2 *Open charm photoproduction*

The main mechanism of open charm production is the photon-gluon fusion: $\gamma g \to \bar{c}c$. This is a direct process and the resolved contribution is expected to be small although in some models it may be substantial. The c quark fragmentation leads to production of charmed particles. Among them the observation of $D^{*\pm}(2.01)$-meson is convenient since its decay

$$D^{*\pm} \to D^0 + \pi^{\pm}, \tag{20}$$

$$D^0 \to K^- + \pi^+, K_s^0 + \pi^+ + \pi^-, K^- + \pi^+ + \pi^+ + \pi^- \tag{21}$$

is characterized by the tight kinematic constraint: $\pi^{\pm}$-meson from $D^{*\pm}$ decay has a definite kinetic energy in the rest frame of D^*.

Measured in the low Q^2 ep-scattering at HERA the event distribution in the mass difference $\Delta M = M(D^0\pi^+) - M(D^0)$ reveals a clear peak at $\Delta M \approx 145.5 MeV$ corresponding to the charmed mesons formation [74, 75]. The mass of D^0-meson was restored in its decays to $K\pi$, $K2\pi$ and $K3\pi$.

H1 and ZEUS studies [76, 77] gave the cross sections of low Q^2 process $ep \to eD^{*\pm}X$ for different Q^2_{max} in the restricted kinematic region of W, $p_T(D^*)$ and $\eta(D^*)$. Measured by ZEUS differential electroproduction cross sections [77] shows discrepancies with NLO QCD calculations [78] in which the parton densities in a proton [67] and in a photon [46] were used. The H1 differential photoproduction cross sections [76] obtained from the electroproduction ones with help of WW approximation [5, 6] are in marginal agreement with NLO QCD [79] but show some excess over the QCD expectations in angular distribution of D^*-mesons in the forward direction.

To derive the integrated over the whole phase space electroproduction cross section the extrapolation of measured values $\sigma(ep \to eD^{*\pm}X)$ should be done. The extrapolation depends on the parton densities in the proton and photon which leads to additional uncertainties in the integrated cross section. The resulting integrated cross section can be converted into the photoproduction cross section and then by using the known fragmentation fraction of c quark to D^{*+} ($B_{c\to D^{*+}} = 0.260 \pm 0.021$ [80]) to the total charm photoproduction cross section $\sigma(\gamma p \to c\bar{c}X)$. Fig.24 shows the HERA results [74, 75, 76] together with the low energy data ($W < 20 GeV$). It is seen that the cross section at HERA energies is an one order

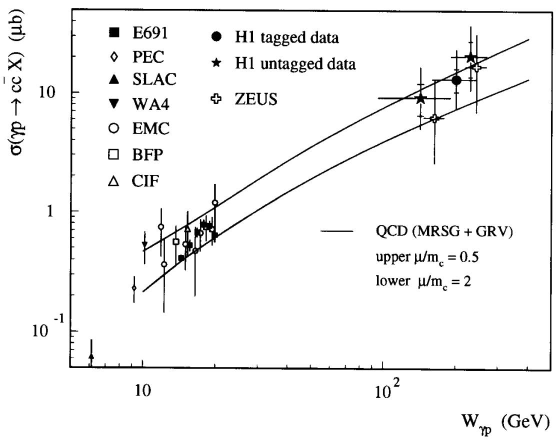

Figure 24: Total charm photoproduction cross section.

of magnitude larger than at $W \approx 20 GeV$. This energy dependence as well as the absolute values of the total charm photoproduction cross section are satisfactory described by NLO QCD for renormalization scale $0.5 \cdot m_c < \mu < 2 \cdot m_c$ [79, 78] (see solid lines in Fig.24).

H1 searched for open charm production in rapidity gap events ($\eta_{max} < 2$) and found evidence of the diffractive production of D^*-mesons [75, 76]. The lower limit for the small Q^2 electroproduction cross section for these RG events $\sigma(ep \to D^{*\pm}X) > 145 pb$ (in the studied kinematical region) is far above the expectations from quark structure of colour singlet exchange in diffractive processes. But this value of σ does not contradict the dominance of hard gluon content of diffractive exchange. This is in line with the results obtained in the study of the hard diffractive photoproduction processes of light quarks (see section 3.4).

5 Conclusions

A bulk of the new data on γp-interactions at HERA was gathered during the last few years. The main results of these investigations of hadron production by almost real photons in earlier non explored energy region up to $W \approx 200GeV$ are:
–The observed slow rise of the total photoabsorption cross section $\sigma_{tot}^{\gamma p}$ with energy W is in accordance with soft pomeron exchange but in contradiction with the mini-jets model prediction of a steep rise;
–The decomposition of $\sigma_{tot}^{\gamma p}$ to diffractive and non-diffractive parts reveals the significant contribution (up to $\approx 40\%$) of soft diffraction;
–The features of soft photoproduction processes are similar to those for hadron reactions (apart from the trivial multiplicative factor in absolute values of cross sections);
–The high p_T inclusive particle spectra in photon induced reactions become harder with increasing W and exhibit the excess over the spectra in hadron induced reaction at corresponding energies which is partly connected with the contribution of *direct* photoproduction process;
–Multiple parton interactions play an important role in hard photon induced reactions;
–The detail study of jet photoproduction processes supports the universality of jet properties;
–The investigation of *direct* and *resolved* photoproduction gives information on the gluon density in a photon and reveals the *anomalous* part in the resolved contribution;
–The study of rapidity gap events shows the presence of hard diffraction in photoproduction processes and gives evidence for a hard gluon content of hard pomeron exchange;
–The observation of interjet rapidity gap events in processes (1) shows a higher rate than in hadron reactions;
–The investigated at HERA of J/ψ and open charm photoproduction exhibited the drastic rise of cross sections with energy and helicity conservation in diffractive J/ψ production;
– The NLO QCD contributions are necessary to explain inclusive spectra, charm production, *etc* in photon induced reactions.

Thus the study of photoproduction processes (1) at HERA has extended the knowledge in soft hadron physics and parton dynamics of hard interactions and improved the theory and phenomenology of γp interactions.

It is not surprising that there are a lot of similarities in photon and hadron induced reactions (both soft and hard) since VDM [1] or underlying parton picture of microphysics leads to this resemblance. Among these similarities there are slow rise of total cross sections at high energies, $1/M_X^2$-dependence of diffractive dissociation cross section, universality of jets properties, phenomena of hard diffraction in hadron and photon reactions, jet structure of hard events and others. The resemblance with hadronic interactions holds also for DIS processes at small x_{Bj} when the distance over which the space-like virtual photon exist as a hadron fluctuation is larger than proton size [81].

On the other hand the specific property of the electromagnetic field to interact with electric charge leads to the peculiarities in photoproduction processes. So called *direct* processes are specific for a photon induced reactions. They are responsible for harder inclusive spectra in photoproduction processes than in a hadron ones. The *anomalous* part of *resolved* contribution which was observed at HERA is also specific only for photoreaction.

As it was mentioned in section 4.1 the cross section of the hard process $\gamma p \to J/\psi p$ exhibits sharp rise with W which is specific for hard diffraction. The hardness is determined also by the Q^2 scale. The study of light vector meson production by virtual photons showed that for $Q^2 > 1GeV^2$ the energy dependence of the elastic cross section is much stronger than for $Q^2 \approx 0$ [8]. Moreover the smooth transition from soft pomeron exchange for real photons to hard pomeron concept (with intercept $\alpha_P(0) \approx 1.2$) for DIS events was observed in the measurements of transverse absorption cross section of virtual photons $\sigma_{T tot}^{\gamma^* p}$. At $Q^2 = 10 - 20GeV$ the cross section is proportional to W^δ with $\delta \approx 0.4$ [64]. Another parameter which determines the hardness of the process is p_T^2 in inclusive spectra. An attempt to observe the change in the dependence of the photoproduction cross section $d\sigma/dp_T^2$ on the energy at different p_T^2 gave the positive results: at higher p_T^2 the W dependence became steeper [82].

Recently the process of prompt photon production in γp-collisions at HERA was observed [83]. The investigation of such reactions opens new possibilities in the study of matter structure at small distances.

6 Acknowledgements

The author thanks Organizing Committee for invitation to attend the Workshop, members of H1 and ZEUS Collaborations for fruitful discussions. It is a pleasure to thank J.Dainton, R.Eichler, B.Levtchenko and R.Nania who read the paper and made valuable remarks, comments and suggestions and N.Lvova for the help in the text preparation. The support of DFG and RFBR is highly appreciated.

References

[1] J.J.Sakurai, Ann.Phys.(NY) **11** (1960) 1.

[2] W.M.Geist et al., Phys.Rept. **197** (1990) 263.

[3] H1 Collab., The H1 Detector at HERA, DESY report 93-103 (1993).

[4] ZEUS Collab., The ZEUS Detector, Status Report 1993, DESY 1993.

[5] C.F. von Weizsäcker, Z.Phys.**88** (1934) 612; E.J.Williams, Phys.Rev. **45** (1934) 729.

[6] V.M.Budnev et al., Phys.Rept. **15** (1975) 181; S.Frixione et al., Phys.Lett. **B319** (1993) 339.

[7] A.Blondel and F.Jacquet, Proceed. of the Study for an ep Facility for Europe, ed. U.Amaldi, DESY 79/48 (1979) 391.

[8] O.Yu.Lukina, these proceedings.

[9] S.I.Alekhin et al., Compilation of cross sections v.4, CERN-HERA-87-01, Feb 1987.

[10] ZEUS Collab., M.Derrick et al., Z.Phys **C63** (1994) 391.

[11] H1 Collab., S.Aid et al., Z.Phys. **C69** (1995) 27.

[12] A.Donnachie and P.V.Landshoff Phys.Lett., **B296** (1992) 227.

[13] R.S.Fletcher, T.K.Gaisser and F.Halzen, Phys.Rev. **D45** (1992) 377.

[14] F.Abe et al., Phys.Rev. **D 50** (1994) 5550.

[15] A.Capella et al., Phys.Lett **B343** (1995) 403.

[16] G.A.Schuler, T.Sjöstrand, Nucl.Phys.**B407** (1993) 539.

[17] E.Gotsman, E.Levin and U.Maor, Phys.Lett **B347** (1995) 424.

[18] H1 Collab., Contribution pa02-067 to 28 ICHEP96, Warsaw, 1996.

[19] ZEUS Collab., Contribution pa02-048 to 28 ICHEP96, Warsaw, 1996.

[20] ZEUS Collab., M.Derrick et al., Z.Phys.**C67** (1995) 227.

[21] R.Hagedorn, Riv. Nouvo Cim. **6** (1983) 1.

[22] T.Sjöstrand and M.Bengtsson, Comp.Phys. Com. **43** (1987) 367; H-U.Bengtsson and T.Sjöstrand, Comp.Phys.Com. **46** (1987) 43; T. Sjöstrand, CERN TH 6488/92 (1992).

[23] M.Erdmann, DESY 96-090, May 1996.

[24] H1 Collab., I.Abt et al., Phys.Lett. **B328** (1994) 176.

[25] OMEGA Photon Collab., R.J.Apsimon et al., Z.Phys. **C43** (1989) 63.

[26] UA1 Collab., C.Albajar et al., Nucl.Phys. **B335** (1990) 261; CDF Collab., F.Abe et al., Phys.Rev.Lett. **61** (1988) 1819.

[27] E.Witten, Nucl.Phys. **B120** (1977) 189.

[28] B.A.Kniehl and G.Kramer, Z.Phys. **C62** (1994) 53.

[29] M.Gluck, E.Reya and A.Vogt, Phys.Rev. **D45** (1992) 3986.

[30] A.D.Martin, W.J.Stirling and R.G.Roberts, Phys.Let. **B306** (1993) 145.

[31] H1 Collab., S.Aid et al., Z.Phys. **C70** (1996) 17.

[32] R.Engel, Z.Phys. **C66** (1995) 203.

[33] ZEUS Collab., M.Derrick et al., Phys.Lett. **B342** (1995) 417.

[34] J.E.Huth et al., FNAL-Conf-90/249-E (1990).

[35] UA1 Collab., C.Albajar et al., Nucl.Phys. **B309** (1988) 405.

[36] H.Abramowich, K.Charchula and A.Levy, Phys.Lett **B269** (1991) 458.

[37] M.Gluck, E.Reya and A.Vogt, Phys.Rev. **D46** (1992) 1973.

[38] ZEUS Collab., M.Derrick et al., Phys.Lett. **B354** (1995) 163.

[39] S.Catani et al., Nucl.Phys. **B406** (1993) 187.

[40] ZEUS Collab., M.Derrick et al., Phys.Lett. **B348** (1995) 665.

[41] ZEUS Collab., Contribution pa02-040 to 28 ICHEP , Warsaw, 1996.

[42] G.Marchesini et al., Comp.Phys.Comm. **67** (1992) 465.

[43] ZEUS Collab., M.Derrick et al., Phys.Lett. **B348** (1996) 401.

[44] H1 Collab., T.Ahmed et al., Nucl.Phys. **B445** (1995) 195.

[45] Ch.Berger and W.Wagner, Phys.Rep. **146** (1987) 1.

[46] M.Gluck, E.Reya and A.Vogt, Z.Phys. **C53** (1992) 127.

[47] H1 Collab., Contribution pa02-080 to 28 ICHEP, Warsaw, 1996.

[48] B.L.Combridge and C.J.Maxwell, Nucl.
Phys. **B239** (1984) 429.

[49] H1 Collab., T.Ahmed et al., Nucl.Phys. **B435** (1995) 3.

[50] P.Bruni and G.Ingelman, DESY 93-187.

[51] ZEUS Collab., M.Derrick et al. Phys.Lett. **B346** (1995) 399.

[52] ZEUS Collab., M.Derrick et al. Phys.Lett. **B356** (1995) 129.

[53] ZEUS Collab., Contribution pa02-039 to 28 ICHEP, Warsaw, 1996.

[54] G.Ingelman and P.E.Schlein, Phys.Lett. **B152** (1985) 256;

[55] J.D.Bjorken, Phys.Rev. **D47** (1993) 101.

[56] ZEUS Collab., M.Derrick et al., Phys.Lett **B369** (1996) 55.

[57] DO Collab., S.Abachi et al., Phys.Rev.Lett **72** (1994) 2332.

[58] CDF Collab., F.Abe et al., Phys.Rev.Lett **74** (1995) 855.

[59] A.Donnachie and P.V.Landshoff, Phys.Lett. **B348** (1995) 213.

[60] H1 Collab., T.Ahmed et al., Phys.Lett. **B338** (1994) 507.

[61] ZEUS Collab., M.Derrick et al., Phys.Lett. **B350** (1995) 120.

[62] ZEUS Collab., Contribution pa02-047 to 28 ICHEP 1996, Warsaw.

[63] H1 Collab., Contribution pa02-085 to 28 ICHEP 1996, Warsaw.

[64] A.Levy, DESY 95-204, November 1995.

[65] M.G.Ryskin, Z.Phys. **C57** (1993) 89.

[66] M.Ryskin at al., RAL-TR-95-065.

[67] A.D.Martin, W.J.Stirling and R.G.Roberts, Phys.Lett. **B354** (1995) 155.

[68] H1 Collab., S.Aid et al., Nucl.Phys. **B472** (1996) 3.

[69] H.Jung et al., Z.Phys. **C60** (1993) 721.

[70] M.Kramer et al., Phys.Lett. **B348** (1995) 657.

[71] M.Kramer, Nucl.Phys. **B459** (1996) 3.

[72] H1 Collab., Contribution pa02-086 to 28 ICHEP 1996, Warsaw.

[73] NA-14 Collab., R.Barate et al., Z.Phys. **C33** (1987) 505.

[74] ZEUS Collab., M.Derrick et al., Phys.Lett. **B349** (1995) 225.

[75] H1 Collab., Contribution EPS-0468 to Europhys. Conf. on HEP, Brussels, 1995.

[76] H1 Collab., S.Aid et al., Nucl.Phys. **B472** (1996) 32.

[77] ZEUS Collab., Contribution pa05-51 to 28 ICHEP, Warsaw, 1996.

[78] S.Frixione et al., Nucl.Phys. **B412** (1994) 225.

[79] S.Frixione et al., Phys.Lett. **B348** (1995) 633; Nucl.Phys. **B454** (1995) 3.

[80] OPAL Collab., R.Akers et al., CERN-PPE/94-217 (1994).

[81] H1 Collab., S.Aid et al., Phys.Lett. **B358** (1995) 412;

[82] H1 Collab., Contribution pa02-79 to 28 ICHEP, Warsaw, 1996.

[83] ZEUS Collab., Contribution pa02-042 to 28 ICHEP, Warsaw, 1996.